13th International Conference on Applications of Statistics and Probability in Civil Engineering, ICASP13
Seoul, South Korea, May 26-30, 2019

Seismic Robustness and Resilience of Structures in the Framework of the JCSS

D.G. Lu
Professor, School of Civil Engineering, Harbin Institute of Technology, Harbin, China

M. Liu
Doctoral candidate, School of Civil Engineering, Harbin Institute of Technology, Harbin, China

M.H. Faber
Professor, Department of Civil Engineering, University of Aalborg, Aalborg, Denmark

ABSTRACT: The awareness of the significance of robustness and resilience of structural systems has gradually intensified over the years. However, robustness and resilience of structures under strong earthquakes have not been paid much attention to in the earthquake engineering community. The great Wenchuan earthquake occurred on May 12, 2008, which caused severe damage and collapse of many structures and huge society costs, have highlighted the importance of robustness and resilience as desirable seismic performance of structures. In this paper, a new framework for engineering risk assessment is applied to evaluate seismic risk of structures, which extends the concept of direct and indirect consequences and associated risks in probabilistic systems modeling formulated by the Joint Committee on Structural Safety (JCSS) to facilitate modeling and analysis of seismic resilience in addition to robustness. The seismic robustness of structures is assessed by a consequence-based index, defined as the ratio between the direct consequences and the total consequences. Moreover, based on recent insights into the modeling of robustness, the quantification of resilience is formulated utilizing a scenario based systems benefit modeling in which resilience failure is associated with exhaustion of the capital accumulated by the system of time. Numerical studies of a simple structural system are performed using the framework and the two new indicators. The relationships of seismic robustness with some other system properties, including over-strength, and redundancy, are investigated, the correlation between robustness and resilience are also shown. The approaches to increasing seismic robustness and resilience of structures are finally suggested.

1. INTRODUCTION

During the service life, structural systems are exposed to natural and man-made hazards, such as earthquakes, typhoons, tornados, floods, fires, snows, ice, malevolent attacks, etc. Recent major earthquakes, especially the great Wenchuan earthquake occurred on May 12, 2008, caused severe damage and collapse of different structures and huge social costs. There has been much research on seismic fragility and vulnerability of structural systems in China, see Lu et al. (2014), and Yu et al. (2017). Recently, due to the challenge of great difficulties of recovery and reconstruction of structures and enormous indirect consequences after earthquakes, structure system properties like robustness and resilience have attracted significant interests. Structural systems in the built environment play significant roles in the sustainable development of society, so not only the engineers, but also the government pay much attentions to robustness and resilience of communities and urbans.

Robustness can be defined in different ways and on different levels of complexity /applicability. Traditionally, in the field of earthquake engineering, robustness has been understood as preventing collapse against strong earthquakes, see Ye et al. (2008). In this paper, a new framework for engineering risk assessment is applied to evaluate seismic risk of structures, which extends the concept of direct and indirect consequences and associated risks in probabilistic systems modeling formulated by the Joint Committee on Structural Safety (Faber (2008) to facilitate modeling and analysis of seismic robustness and resilience of structures. There are various methods to model seismic resilience of structures (Cimellaro et al. (2010) and Ouyang et al. (2012)). However, most references are concentrating on single time disturbance and the associated recovery process. In this paper, a more holistic method proposed by Faber et al. (2017) is used to assess structural system resilience under earthquakes.

In this paper, the probabilistic modeling method for system failure and failure consequences in the framework of the JCSS is introduced to facilitate modeling and analysis of seismic robustness and resilience of structures. Based on the scenario modeling framework, the modeling method for structural robustness is introduced and the robustness index is defined in two different ways. Furthermore, the resilience modeling method is introduced to quantify seismic resilience of structures considering the life-cycle benefit. Finally, the seismic robustness and resilience of a simple frame considering the associated governance system are investigated, the approaches to increasing seismic robustness and resilience of structures are suggested and further research suggestions are also proposed.

2. PROPOSED FRAMEWORK AND PROBABILISTIC MODELING APPROACH

2.1. Probabilistic modeling of earthquakes

To analyze seismic robustness and resilience of structures, the occurrence of earthquake events is modeled by homogeneous Poisson process, and the intensity of the earthquake loads are modeled by log-normal distribution, see Figure 1. The resistance of each constituent with respect to the earthquake events are represented by its bending strength capacity, see Figure 2.

2.2. Modeling framework of system failures

The system of consideration is assumed to have n_c constituents which may fail individually and in combinations due to a combination of external and internal demands. The failure of a system is modelled as a two-phase phenomenon as illustrated in Figure 3.

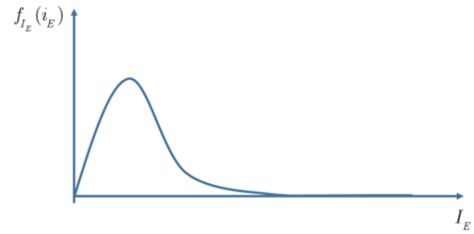

Figure 1: Illustration of earthquake load intensity.

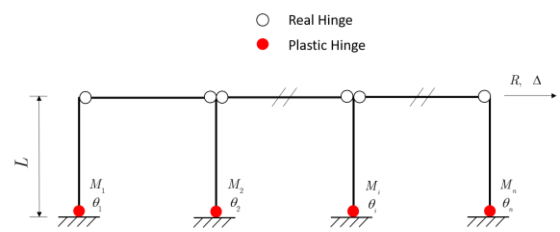

Figure 2: Illustration of earthquake effects.

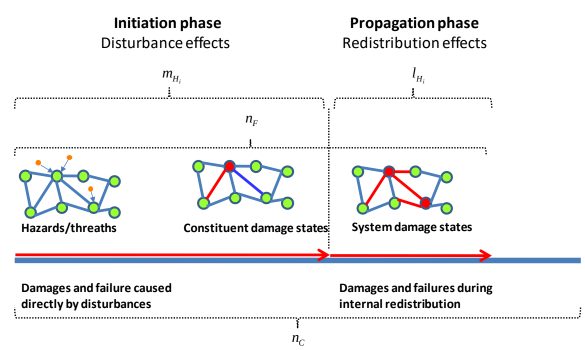

Figure 3: Illustration of the two phase scenario based failure propagation model.

2.3. Individual and cascading failures in the initiation and propagation phases

In the initiation phase, see Figure 3, an earthquake causes failures of constituents. Following these failures - in the propagation phase - the demands of the constituents of the system are redistributed until both internal and external demands are in equilibrium with the capacity of the system or until the system totally fails. This process may occur in a sequence of failures and subsequent redistributions – denoted as cascading failure. It is assumed that in total $n_{f,p}$ constituents fail during the propagation phase. If after the propagation phase the total number of failed constituents is $n_f = n_{f,i} + n_{f,p} = n_c$, then the system totally fails.

2.4. Consequence modeling

The consequences following failures of constituents are differentiated into two principal categories, namely direct and indirect (or follow-up) consequences, i.e., C_D and C_{ID} respectively, see also Figure 4.

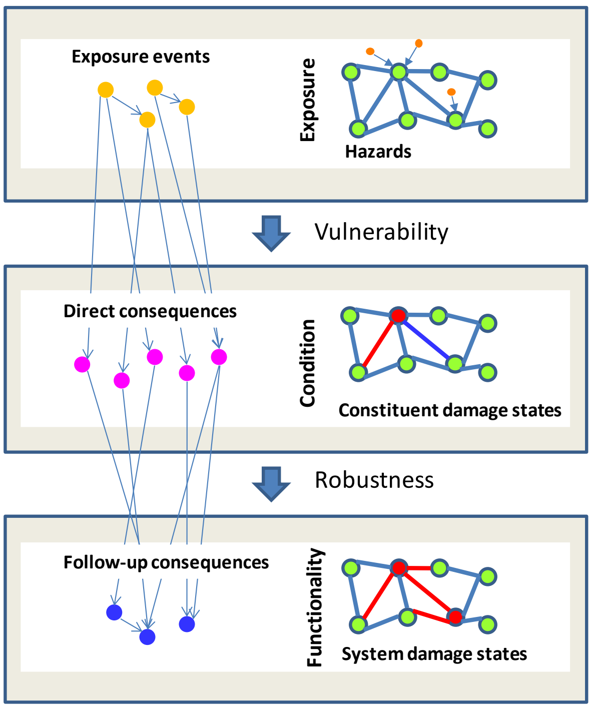

Figure 4: Illustration of the modelling of consequences associated with system damage and failure scenarios.

Loss of constituents may or may not be associated with loss of system services. Direct consequences are most often associated with individual constituent failures, whereas indirect consequences are associated with loss of system functionality and services caused by individual failures as well as combinations of constituent failures.

2.5. Seismic robustness modeling

Based on the scenario modeling framework outlined in the foregoing, we herein assume that it is possible to identify a probabilistic representation of all possible or relevant scenarios of constituent failures associated with consequences. If the system is comprised by n_C constituents there are in principle m different scenarios, i.e.

$$m = \sum_{k=1}^{n_c} \binom{n_c}{k} = n_c^2 - 1 \tag{1}$$

which may be associated with direct and indirect consequences of failures.

The probabilistic characterization of these scenarios may be given in the following form:

$$S_i = (p(i), n_{f,i}, (i), C_{DI}(i), n_{f,p}, C_{DP}(i), C_{ID}(i)),\ i = 1,2,..,m \tag{2}$$

Obviously, from Eq. (1) the number of different scenarios may be overwhelmingly large even for systems comprised by a moderate number of constituents. It is thus a central, critical and rather non-trivial issue to be able to identify the scenarios which are relevant and of significance for the generation of consequences. To efficiently identify the individual scenarios necessitates a joint consideration of their probabilities and consequences. The assessment of their probabilities typically necessitates the probabilistic analysis of unions of intersections of failure events – with due account of dependencies between these. Moreover, it should be highlighted that in practical engineering applications some of the mathematically possible scenarios may be irrelevant or physically impossible and must be excluded in the modelling.

The understanding and modelling of the physical characteristics of the considered systems thus play significant roles for systems reliability analysis and different techniques for this have emerged in different application areas. In this connection it should be mentioned that the branch-and-bounding and beta-unzipping methods, see Thoft-Christensen and Murotsu

(1986), appear to have some general merits in the identification of relevant systems failure scenarios across application domains, see e.g. Qin (2012).

Based on the probabilistic scenario representation provided in Eq. (2), we may define the index of robustness in two different ways. If we are particularly interested in understanding to what degree the system is able to limit the direct consequences to the direct consequences occurring in the initiation phase, then the robustness index I_{R_1} might be assessed as:

$$I_{R_1}(i) = \frac{C_{DI}(i)}{C_{DI}(i) + C_{DP}(i)} \tag{3}$$

An alternative robustness index I_{R_2} expressing the ability of the system to limit the number of failed constituents to those occurring in the initiation phase may be expressed as:

$$I_{R_2}(i) = \frac{n_{f,i}(i)}{n_{f,i}(i) + n_{f,p}(i)} \tag{4}$$

Finally, we might also express the system's ability to limit total consequences to direct consequences through the robustness index

$$I_{R_3}(i) = \frac{C_{DI}(i) + C_{DP}(i)}{C_{DI}(i) + C_{DP}(i) + C_{ID}(i)} \tag{5}$$

2.6. Seismic resilience modeling

The resilience model proposed in Faber et al. (2017) is illustrated in Figure 5. As shown in Figure 5, the dash line represents the economic capacity. In this study, it is assumed that the economic capacity is generated by accumulating a fixed percentage χ % of the annual benefit. It is assumed that a startup capacity is available at time $t = 0$ (χ % of the total benefit generated in the whole service life). When an earthquake causes system damage or failure, the system economic reserve would be reduced for the cost of recovery. System resilience failure is then defined as the exhaustion of the system reserve (see green dash line in Figure 5):

$$g_{\mathrm{RF}}(\mathbf{X}(t), \mathbf{a}) = R_r(\mathbf{X}(t), \mathbf{a}) - S_r(\mathbf{X}(t), \mathbf{a}) \tag{6}$$

where R_r and S_r are functions representing the capacity and the demand of the system at time t, respectively.

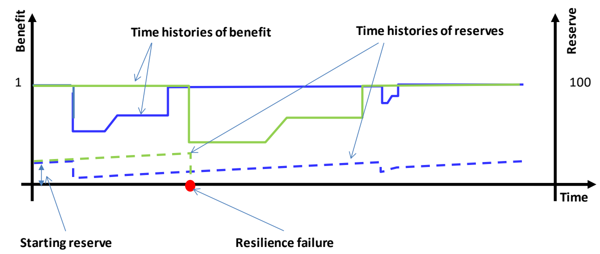

Figure 5: Illustration of resilience model in terms of evolution of benefit and corresponding evolution of accumulated reserves with time (Faber et al. (2017)).

3. CASE STUDY

In the following case study, the seismic robustness and resilience of a simple frame structure (see Figure 2) is investigated and the relationships of seismic robustness and resilience together with other system properties, including system safety factor and redundancy, are analyzed in accordance with the framework and the approach outlined in Section 2.

The case study model can be modeled by a Daniels system which is comprised of n_C constituents, see Figure 6.

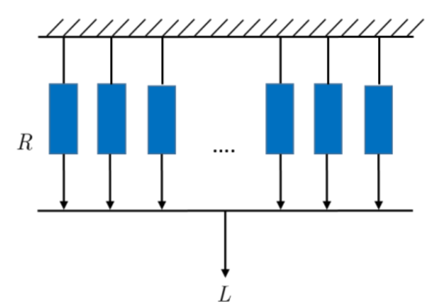

Figure 6: Schematic of the numerical example.

In Figure 6, $M_u = R_i$ (i=1,2,…, n_C) is the bending strength capacity of each member, and L is represented as the earthquake load.

The distribution parameters of R_i and L are provided in Table 1.

Table 1: Distribution parameters for R_i and L.

Variable	*Distribution*	*Mean*	*CoV*
R_i	*normal*	SSF/n_C	*0.2*
L	*log-normal*	*1*	*0.8*

In Table 1, SSF is represented as the system safety factor, which is defined as over-strength factor by Bertero and Bertero (1999), can be computed as:

$$SSF = \frac{\mu_R}{\mu_D} \tag{7}$$

3.1. Seismic robustness analysis results

In this study, a system of up to 20 constituents is considered and each constituent is assumed to behave brittle at failure, implying that they lose their carrying capacity completely after their capacity limits are reached.

The robustness index introduced above is used to analyze seismic robustness of the considered case-study structure. Here the direct consequences are calculated as the replacement costs associated with constituent failures due to the earthquake load (before internal load redistribution), while the indirect consequences are associated with replacement due to failure caused by internal load redistribution (see Eq. (3)). Figures 7−8 show how the index of robustness change with the variation of the number of constituents and system safety factor.

It can be found from Figures 7-9 that raising n_C and SSF has remarkable influences on robustness index when the probability of system failure is high. The reason for this is that systems with fewer constituents or lower SSF are more prone to failure when constituent failures take place.

To analyze the distribution of the number of failed constituents, we choose two systems with 5 and 10 constituents respectively, then the number of failed constituents generated by 10^6 Monte Carlo Simulation is counted, see Figure10.

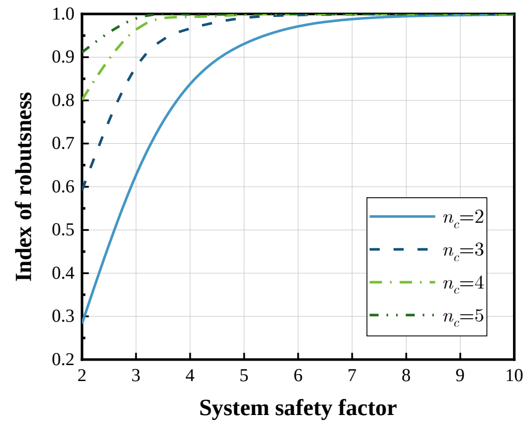

Figure 7: Index of robustness versus SSF, for four values of the number of constituents.

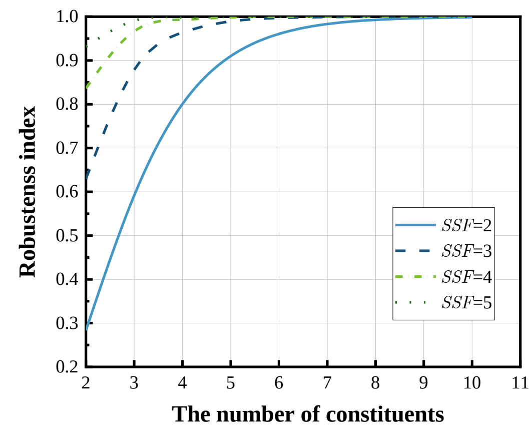

Figure 8: Index of robustness versus n_C, for four values of the system safety factor.

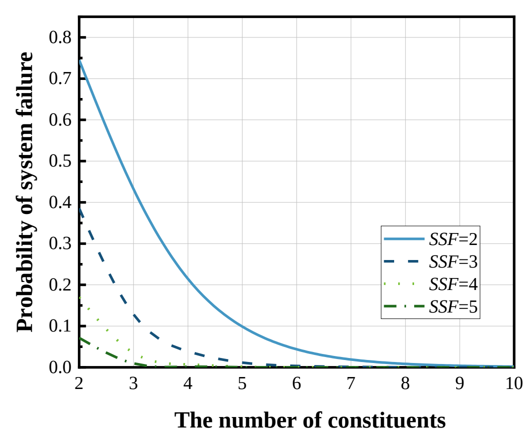

Figure 9: Probability of system failure.

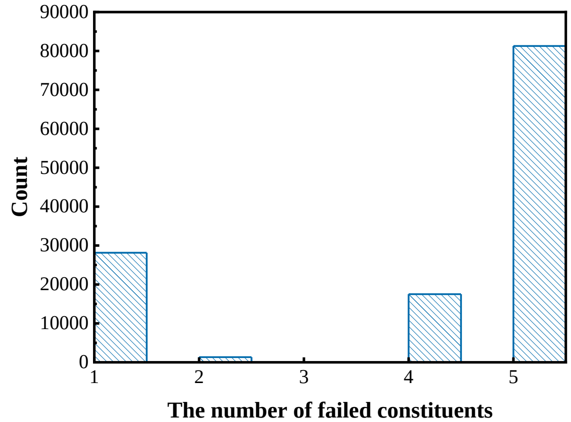

(*a*) n_C =5

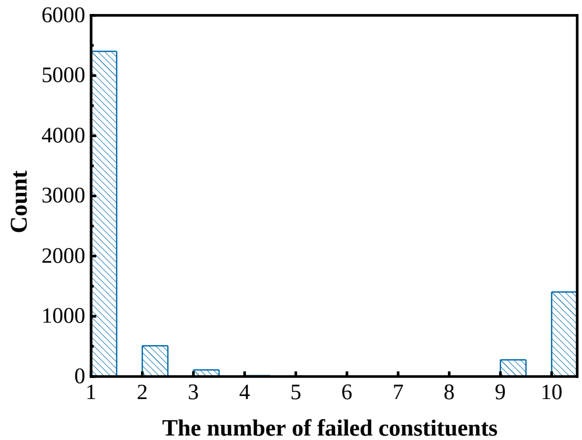

(*b*) n_C =10

Figure 10: Distribution of the number of failed constituents for 10^6 *Monte Carlo Simulation when* n_C *=5 and* n_C *=10, SSF=2.*

It can be observed from Figure 10 that the counts at both ends of the x-axis are dramatically higher than that in the middle. It can be inferred that the abilities of redistribution for this two systems are low. The reason is that the resistance of each constituent is set to follow the same distribution in the present example, which can lead to that most of the constituents are in the same state.

3.2. Seismic resilience analysis results

To analyze the seismic resilience of structures, earthquake disturbances are assumed to follow a Poisson process with an annual occurrence rate $\lambda_H = 1/50$. The distribution parameters of the intensity can be found in Table 1. The service life of the considered structure is set to be 50 years.

During the entire service life, the total benefit of the considered structure is influenced by earthquake loads. Here the governance system is used to describe the change of benefit and structural reorganization as well as recovery time, see Figure 11.

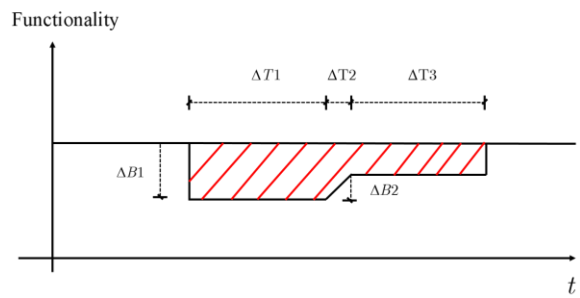

Figure 11: Illustration of the representation of the performance of the governance system with respect to reorganization and recovery of the structure functionality after disturbance.

Figure 11 shows how the functionality of the structure changes after the disturbance of an earthquake. At the time of the earthquake event happens, the functionality of this structure is reduced by ΔB_1, in this study it is assumed to be proportional to the number of constituents failure, i.e. $\Delta B_1 = n_F / n_c$. ΔT_1 represents the time till the governance system has established an overview of the situation and initiates commission of temporary measures to re-establish functionality. The temporary measures are assumed to be fully functional after a period ΔT_2 with a resulting functionality gain equal to ΔB_2. In parallel to and after commissioning of temporary measures it is assumed that the permanent measures for re-establishing functionality are being planned and prepared. These are assumed commissioned after a period ΔT_3.

The distribution parameters for ΔT_i are provided in Table 2.

Table 2: Distribution parameters for ΔT_i .

Preparedness level	*Variable*	*Distribution*	*Mean*	*CoV*
Low	ΔT_1	*Log-normal*	ΔB_1	*0.2*
	ΔT_2	*Log-normal*	$5\Delta B_1$	*0.2*
	ΔT_3	*Log-normal*	$20\Delta B_1$	*0.2*
	ΔB_1	*Deterministic*	n_F / n_c	
	ΔB_2	*Deterministic*	$0.5\times\Delta B_1$	
High	ΔT_1	*Log-normal*	$0.5\times\Delta B_1$	*0.1*
	ΔT_2	*Log-normal*	ΔB_1	*0.1*
	ΔT_3	*Log-normal*	$10\Delta B_1$	*0.1*
	ΔB_1	*Deterministic*	n_F / n_c	
	ΔB_2	*Deterministic*	$0.8\times\Delta B_1$	

In this example, the annual benefit generated by each constituent is assumed to be 12, then the total benefit for the whole service life is calculated. Figure 12 shows the total benefit for the considered systems under two levels of preparedness. It is apparent that the systems under high preparedness generate more benefits than those under low preparedness. It can also be observed that increasing SSF improves the total benefit.

The cost of recovery is assumed to be proportional to the number of constituent failures, i.e. $30n_F$. Following the seismic resilience modeling method introduced above, the probabilities of resilience failure (P_{RF}) can be calculated, see Figures 12 and 13. To compare, we choose four systems which comprise 5, 10, 15, 20 constituents, respectively. In this example, the system safety factor is set to be 1 to increase the probability of system failure and the regularity can be observed more clearly. The probabilities of resilience failure are calculated as a function of the decision parameter χ which refers to the amount of annual benefit transferred to a financial reserve. It can be observed from Figures 13 and 14 that χ has significant effects on the probabilities of resilience failure especially when n_C is small. Due to the low annual occurrence rate of the earthquake, the level of preparedness is not of significant influence, but it can be observed from Figure 14 that the probability of resilience failure under high preparedness is lower than that under low preparedness, which has a substantial effect on consequences.

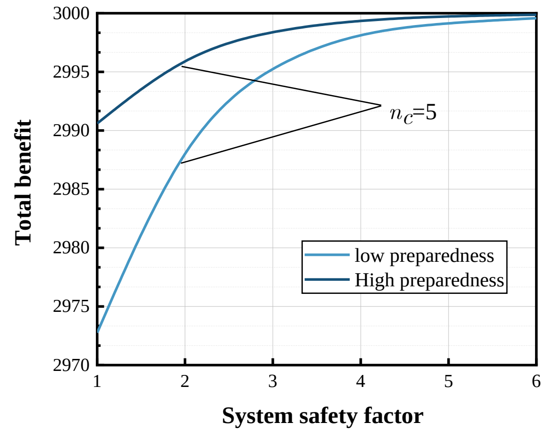

(*a*) *Total benefit for system with 5 constituents*

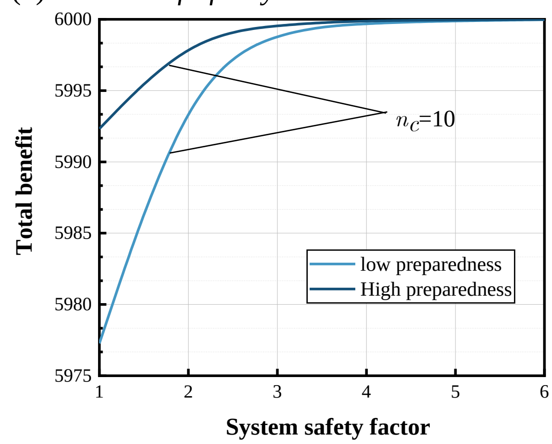

(*b*) *Total benefit for system with 10 constituents*

Figure 12: Comparison of the total benefit under high/low preparedness as a function of SSF.

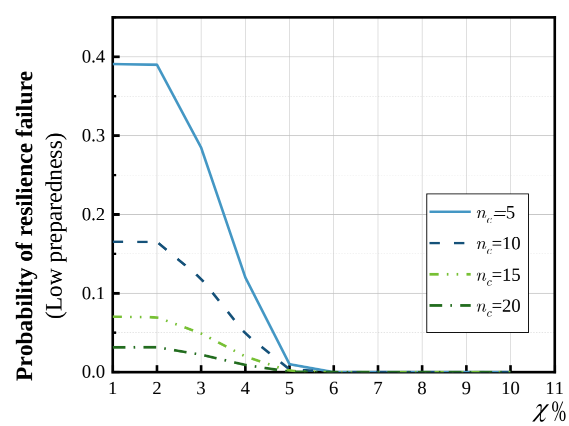

(*a*) P_{RF} *under low preparedness*

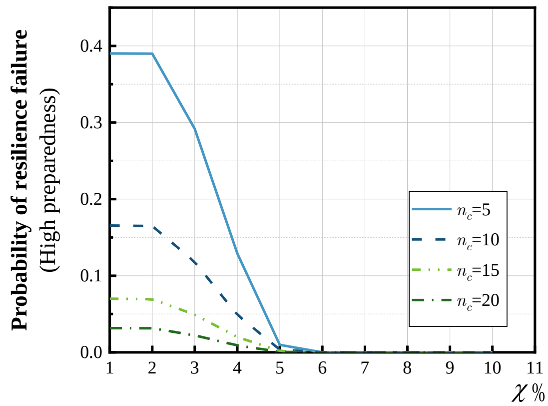

(b) P_{RF} *under high preparedness*

Figure 13: Comparisons of the probability of resilience with the variation of the percentage χ *% for four values of the number of constituents.*

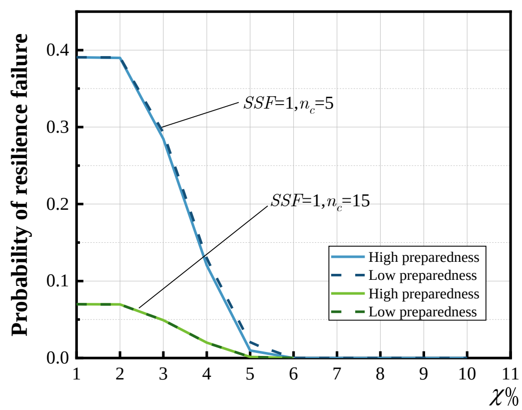

Figure 14: Comparisons of the probability of resilience failure for two level of preparedness.

4. CONCLUSIONS

In this paper, a probabilistic modeling framework for the assessment of seismic resilience and robustness of structures is presented. The modeling methods of system failure and failure consequence modeling are introduced to facilitate assessment of seismic robustness and resilience of structures. Resilience failure is modeled as a function of the decision parameter, which can support resilience management. A simple frame structure is used to investigate the relationships of seismic robustness and resilience together with other system properties, including over-strength and redundancy. The example shows how robustness and resilience failure change with different systems, which can provide references for structural design and decision making.

The modeling method for seismic robustness and resilience needs to be extended to consider more structural properties such as correlation of constituent resistance, resistance deterioration, and so on. However, this framework is adaptable and more details can be added to apply it to various scenarios.

5. REFERENCES

Bertero, R. D., and Bertero, V. V. (1999). "Redundancy in earthquake-resistant design." *Journal of Structural Engineering*, 125(1), 81-88.

Cimellaro, G. P., Reinhorn, A. M., and Bruneau, M. (2010). "Framework for analytical quantification of disaster resilience." *Engineering Structures*, 32(11), 3639-3649.

Faber, M. H. (2008). "Risk Assessment in Engineering: Principles, System Representation & Risk Criteria." ETH Zurich.

Faber, M. H., Qin, J., Miraglia, S., and Thöns, S. (2017). "On the probabilistic characterization of robustness and resilience." *Procedia Engineering*, 198, 1070-1083.

Lu, D. G., Yu, X. H., Jia, M. M., and Wang, G. Y. (2014). "Seismic risk assessment for a reinforced concrete frame designed according to Chinese codes." *Structure and Infrastructure Engineering*, 10(10), 1295-1310.

Ouyang, M., Dueñas-Osorio, L., and Min, X. (2012). "A three-stage resilience analysis framework for urban infrastructure systems." *Structural Safety*, 36-37(2), 23-31.

Qin, J. (2012). "*Probabilistic Analysis of Large-scale Engineering Systems.*" ETH Zurich.

Thoft-Christensen, P., and Murotsu, Y. (1986). *Application of Structural Systems Reliability Theory*, Springer-Verlag.

Ye, L. P., Cheng, G. Y., Lu, X. Z., and Feng, P. (2008). "Introduction of robustness for seismic structures." *Building Structures*, (in Chinese).

Yu, X. H., Lu, D. G., and Li, B. (2017). "Relating seismic design level and seismic performance: fragility-based investigation of RC moment-resisting frame buildings in China." *Journal of Performance of Constructed Facilities*, 31(5), 04017075.